ISSN: 0067-2904
GIF: 0.851

Investigation of the Nuclear Structure of $^{174-206}$Hg Isotopes Using Skyrme-Hartree-Fock Method

R. A. Radhi*, Ali A. Alzubadi, Nabeel F. Latooffi
Department of Physics, College of Science, Baghdad University, Baghdad Iraq.

Abstract

The effective Skyrme type interactions have been used in the Haretree-Fock mean-field model for several decades, and many different parameterizations of the interaction have been realized to better reproduce nuclear masses, radii, and various other data. In the present research, the SkM, SkM*, SI, SIII, SIV, T3, Sly4, Skxs15, Skxs20 and Skxs25 Skyrme parameterizations have been used within Haretree-Fock (HF) method to investigate some static and dynamic nuclear ground state properties of $^{174-206}$Hg isotopes. In particular, the binding energy per nucleon, proton, neutron, mass and charge densities and corresponding root mean square radii, neutron skin thickness and charge form factor. The calculated results are compared with the available experimental data. From present calculation, we can deduce that the Skyrme–Hartree–Fock (SHF) method with above parameterizations provide a good description on the Hg isotopes.

Keywords: Skyrme interaction, Skyrme-Hartree-fock method, Hg-isotopes.

دراسة التركيب النووي للنظائر $^{174-206}$Hg باستخدام طريقة سكيرم–هاريتري–فوك

رعد عبد الكريم راضي*، علي عبد اللطيف الزبيدي، نبيل فوزي لطوفي
قسم الفيزياء، كلية العلوم، جامعة بغداد، بغداد، العراق.

الخلاصة

يتناول هذا البحث دراسة التركيب النووي لبعض نظائر الزئبق $^{174-206}$Hg من خلال حساب خواص الحالة الارضية لها مثل كثافة كل من الشحنة، البروتون، النيوترون والكتلة مع انصاف الاقطار المرافقة لها و كذلك حساب السمك النيوتروني، طاقات الربط، وعوامل تشكل الشحنة. تم استخدام طريقة سكيرم هارتري فوك في تنفيذ هذه الدراسة مع باراميترات مختلفة وهي SkM, SkM*, SI, SIII, SIV, T3 Sly4, Skxs15, Skxs20, Skxs25 Skyrme. لقد تمت دراسة تاثير هذه البارامترات المختلفة على خواص النظائر المذكورة اعلاه وذلك لتحديد اي من هذه البارامترات يحقق افضل تطابق مع الحسابات العملية لتلك الخواص. ويستنتج من هذه الدراسة ان طريقة سكيرم هارتري فوك تعطي وصف جيد لخواص هذه النظائر. كما تمت المقارنة بين النتائج النظرية والتجريبية لعوامل تشكل الشحنة.

Introduction

The mean field theory is widely used, in various modifications, as a base for practically all microscopic calculations in many body quantum systems. In nuclear physics, it is essentially an approximated scheme to reduce our problem of many strongly interacting nucleons to one of non-interacting particles in an average nuclear field. The generation of this average field from the nucleon-

*Email:Raaed radhi@yahoo.com

nucleon interaction in a self-consistent way is achieved by the Hartree-Fock (HF) method. Different forms of a phenomenological interaction are used for this purpose. The Skyrme force to be used in the present research is among those most important and most widely utilized phenomenological force used with the HF method [1]. The Skyrme-Hartree-Fock (SHF) model has enjoyed enormous success in providing an appropriate description of the ground-state properties of both stable and unstable nuclei since the implementation of the Skyrme interaction [2-4]. It incorporates the essential physics in terms of a minimal set of parameters, e.g., an *s*- and *p*-wave expansion of an effective nucleon–nucleon interaction together with a density dependent part which accounts for the truncation of the shell–model space to a closed-shell configuration as well as for three-body interactions. A common trend of phenomenological interactions used in the mean field approach is their simple mathematical structure. It has mathematically a zero range; however, velocity dependent terms mock up the finite range of the nuclear force. This allows writing the nuclear part of the HF energy as a functional of *local* one-body densities only, and the HF equations take the form of simple Schrödinger equations with local mean fields [5].

The structure of a nucleus can be described in nuclear physics by calculating some of the basic quantities such as various nuclear densities and the associated root-mean-square (rms) radii, the neutron-skin thickness and charge form factor. Nuclear charge density distribution gives us much detailed information on the internal structure of nuclei since they are directly related to the wave functions of protons, which are important keys for many calculations in nuclear physics [6, 7].

In the present research, we will investigate some static and dynamic ground state properties of $^{174-206}$Hg isotopes using ten typical parameterizations of SKM, SKM*, SI, SIII, SVI, TIII, Sly4, Skxs15, Skxs20 and Skxs25 [8-14].

Theory

The effective interaction proposed by Skyrme was designed for HF calculations of nuclei [15, 16]. It is the most convenient force used in the description of the ground states properties of nuclei with about ten adjustable parameters which obtained by fitting the experimental data of nuclei, such as binding energies and charge radii [17]. The Skyrme forces are zero-range interactions, it's basically consists of a two-body term which is momentum dependent and a zero range three-body term. In the HF calculations, the three-body term can be replaced with a density-dependent two-body term. Thus, the Skyrme forces are unified in a single form as an extended Skyrme force [18]. The two-body Skyrme interaction is written as follows [15]:

$$\begin{aligned} v_{12} &= t_0\left(1+x_0\hat{P}_\sigma\right)\delta(r_1-r_2) \\ &+\frac{1}{2}t_1\left(1+x_1\hat{P}_\sigma\right)\left(\hat{k}^2\delta(r_1-r_2)+\delta(r_1-r_2)\hat{k}'^2\right) \\ &+t_2\left(1+x_2\hat{P}_\sigma\right)\hat{k}^2.\delta(r_1-r_2)\hat{k}+\frac{1}{6}t_3\left(1+x_3\hat{P}_\sigma\right)\rho^\alpha(\vec{R})\delta(r_1-r_2) \\ &+iW_0\hat{k}'(\hat{\sigma}_1+\hat{\sigma}_2)\times\hat{k}\delta(r_1-r_2), \end{aligned} \quad (1)$$

where $R=\frac{r_1+r_2}{2}$ and α are the Skyrme force parameters. The $\hat{k}=\left(\vec{\nabla}_1-\vec{\nabla}_2\right)/2i$ and $\hat{k}'=-\left(\vec{\nabla}_1'-\vec{\nabla}_2'\right)/2i$ operators are the relative wave vectors of two nucleons acts to the right and to the left (*i.e.* the complex conjugate wavefunctions, with coordinate r') respectively. The terms t_0, $t_1, t_2, t_3, x_0, x_1, x_2, x_3$ and W_0 are the free parameters describing the strengths of the different interaction terms which are fitted to the nuclear structure data. $\hat{P}_\sigma$ is spin-exchange operators. $\delta(r_1-r_2)$ is the delta function, and σ is the vector of Pauli spin matrices.

The total-energy density of a nucleus in the standard SHF model, is written as [19]

$$E=E_{kin}+E_{Sky}+E_{Coul}+E_{pair}+E_{cm}, \quad (2)$$

where E_{kin} is the kinetic energy of the nucleons (proton and neutron) and can be given by the following relation [20]:

$$E_{kin}=\sum_{i=1}^{A}\frac{\hbar^2}{2m_i}\int\tau_i d^3r \quad (3)$$

E_{Sky} is the energy functional of the Skyrme force and given by:

$$E_{Sky} = \int d^3r \left[\frac{b_0}{2}\rho^2 - \frac{b_0'}{2}\sum_q \rho_q^2 + \frac{b_3}{3}\rho^{\alpha+2} - \frac{b_3'}{3}\rho^{\alpha}\sum_q \rho_q^2 + b_1\rho\tau \right.$$
$$\left. -b_1'\sum_q \rho_q\tau_q - \frac{b_2}{2}\rho\Delta\rho + \frac{b_2'}{2}\sum_q \rho_q\Delta\rho_q - b_4\rho\nabla\cdot J - b_4'\sum_q \rho_q\nabla\cdot J_q \right] \quad (4)$$

where ρ_q is the local densities for protons and neutrons (depending on the value of q), ρ the total density, τ_q is the kinetic energy densities for protons and neutrons and J_q is the spin-orbit current density. They are given by these relations [3]:

$$\rho_q(r) = \sum_{i\sigma} |\phi(r,\sigma,q)|^2 \quad , \quad \tau_q(r) = \sum_{i\sigma} \left|\vec{\nabla}\phi(r,\sigma,q)\right|^2 ,$$
$$J_q(r) = -i \sum_{i\sigma\sigma'} \phi_i^*(r,\sigma,q)[\nabla\phi_i(r,\sigma',q) \times \langle\sigma|\hat{\sigma}|\sigma'\rangle] \quad (5)$$

The parameters in the energy Skyrme equation are given by:

$$b_0 = t_0\left(1+\frac{1}{2}x_0\right), \quad b_0' = t_0\left(\frac{1}{2}+x_0\right)$$
$$b_1 = \frac{1}{2}\left[t_1\left(1+\frac{1}{2}x_1\right) + t_2\left(1+\frac{1}{2}x_2\right)\right]$$
$$b_1' = \frac{1}{2}\left[t_1\left(\frac{1}{2}+x_1\right) - t_2\left(\frac{1}{2}+x_2\right)\right]$$
$$b_2 = \frac{1}{8}\left[3t_1\left(1+\frac{1}{2}x_1\right) - t_2\left(1+\frac{1}{2}x_2\right)\right]$$
$$b_2' = \frac{1}{8}\left[3t_1\left(\frac{1}{2}+x_1\right) + t_2\left(\frac{1}{2}+x_2\right)\right]$$
$$b_3 = \frac{1}{4}t_3\left(1+\frac{1}{2}x_3\right), b_3' = \frac{1}{4}t_3\left(\frac{1}{2}+x_3\right). \quad (6)$$

The third part of the total energy equation is the Coulomb energy part. There is a small contribution to the Coulomb energy coming from the exchange part. This contribution is due to the fact that the Coulomb interaction is infinite range [2, 21]. The Coulomb energy is given by:

$$E_{Coul} = \frac{e^2}{2}\iint \frac{\rho_p(\vec{r})\rho_p(\vec{r}')}{|\vec{r}-\vec{r}'|} d^3r d^3r' + E_{Coul,exch} \quad (7)$$
$$E_{Coul,exch} = -\frac{3}{4}e^2\left(\frac{3}{\pi}\right)^{1/3} \int \rho_p(r)^{4/3} dr \quad (8)$$

It is possible to constitute, from the single particle wave function determined by the HF calculation, the nucleon densities $\rho_p(r)$ and $\rho_n(r)$. In the Skyrme–Hartree–Fock (SHF) theory using the Skyrme forces, the most general product wave functions (ψ_β) consist of independently moving single particles. In this method the neutron and proton densities are given in [22]:

$$\rho_q(\vec{r}) = \sum_i |\varphi_i(r)|^2 = \sum_\beta w_\beta \frac{2j_\beta+1}{4\pi}\left(\frac{R_\beta}{r}\right)^2 \quad (9)$$

Here, q denotes the neutron or proton and w_β represents the occupation weight of single-particle levels. The completely filled shells have $w_\beta = 1$, but fractional occupancies occur for nonmagic nuclei. We restrict to consider the ground state of spherical nuclei. R_β are the redial parts of the wave function and j_β I the angular momentum.

The root-mean-square (rms) radii of neutron, proton, charge and mass distributions can be evaluated from these density distributions by [23]:

$$r_q = \langle r_q^2\rangle^{1/2} = \left[\frac{\int r^2\rho_q(r)dr}{\int \rho_q(r)dr}\right]^{1/2} \quad (10)$$

where q represent neutron, proton, charge and mass.
A quantity of both theoretical and experimental interest, the neutron skin thickness t, is a very sensitive probe of the pressure difference that exists between neutrons and protons in the atomic nucleus. In nuclei it may be defined as the difference between the neutron and proton diffraction radii

$$t = \langle r^2 \rangle_n^{1/2} - \langle r^2 \rangle_p^{1/2} \qquad (11)$$

The proton and neutron densities from the HF method with the intrinsic charge density of the nucleons can be calculating by a simple product in Fourier space, so that it is transformed the densities to the so-called form factors [24]

$$F_{ch}(q) = 4\pi \int_0^{\infty} dr\, r^2 j_0(qr) \rho_{ch}(r) \qquad (12)$$

where q is the momentum transfer, and $j_0(qr) = sin(qr)/qr$ is the spherical Bessel function of zeroth order. The normalization in Equ. (17) was chosen to give $F_{ch}(q = 0) = 1$

Results and Discussion

The Skyrme parameterizations that have been used in the present research were tabulated in Table-1. We first calculate binding energies, the charge rms radii, and the neutron Skin thickness, then the charge, proton, neutron and mass densities are presented using the best Skyrme parameterization which is given the best reproducing for the binding energy data. These calculations are followed by the investigation of the longitudinal form factor for the Hg isotopes using the same Skyrme parameterizations mentioned above.

Figure-1 (a and b) shows the charge density profiles obtained with the investigated Skyrme parameterizations used in this work as well as the experimental charge distributions for [25] ^{204}Hg. Theoretically the calculated charge density values are quite consistent with the theoretical calculations with all the Skyrme parameterizations. In general, theoretical and experimental charge densities agree nicely in the fall-off region and differ more in the nuclear interior as a consequence of the shell oscillations of the mean-field densities specially for (SkM*, SkM, SI, SIII, SVI). For the other Skyrme parameterizations the theoretical calculations coincide with the experimental data for all the range of r (fm).

Table 1-The Skyrme parameterizations that have been used in the present research.

Force	t_0	t_1	t_2	t_3	W_0	x_0	x_1	x_2	x_3	α
SkM	−2645.0	385.0	−120.0	15 595.0	130	0.09	0.0	0.0	0.0	1/6
SkM*	−2645.0	410.0	−135.0	15 595.0	130	0.09	0.0	0.0	0.0	1/6
SI	−1057.3	235.9	−100.0	14 463.5	0.0	0.56	0.0	0.0	1.0	1.0
SIII	−1128.75	395.0	−95.00	14 000.0	120	0.45	0.0	0.0	1.0	1.0
SVI	−1101.81	271.67	−138.33	17 000.0	115	0.583	0.0	0.0	1.0	1.0
TIII	−1791.80	298.50	−99.05	12 794.0	126	0.138	−1.0	1.0	0.075	1/3
SLy4	−2488.90	486.80	−546.30	13777.00	161.35	123.00	0.83400	−0.3440	1.35400	1/6
Skxs15	−2883.29	291.60	−314.89	18239.55	161.35	0.4762	−0.25433	−0.61109	0.52936	1/6
Skxs20	−2885.24	302.73	−323.42	18237.49	162.73	0.13746	−0.25548	−0.60744	0.05428	1/6
Skxs25	−2887.81	315.50	−329.30	18229.81	163.93	−0.18594	−0.24766	−0.60119	−0.40902	1/6

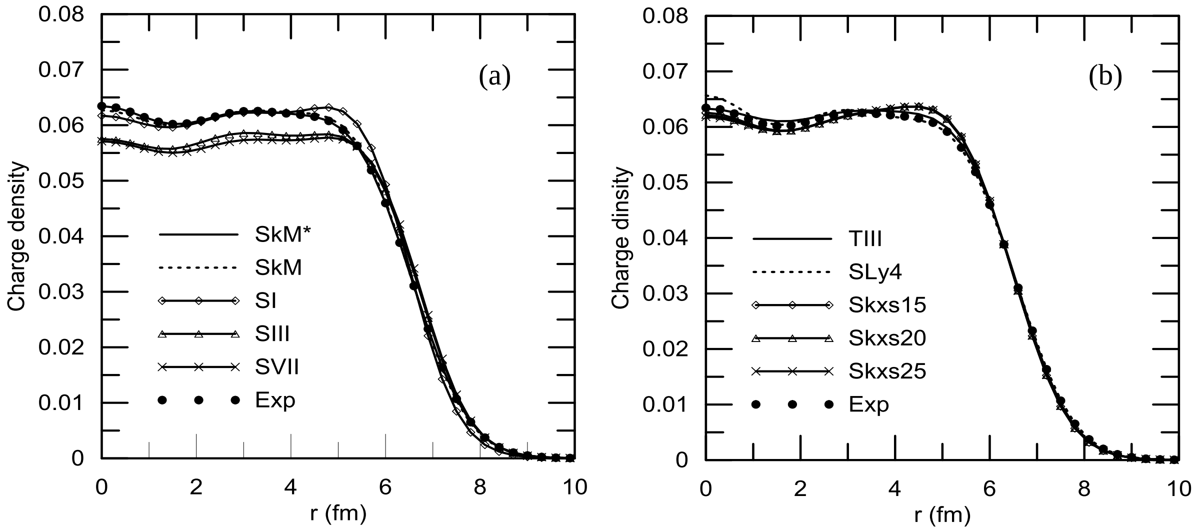

Figure 1- Charge density distribution for ^{204}Hg using different Skyrme parameterizations.

Since the nucleons themselves have intrinsic electromagnetic structure, the proton and neutron densities have been studied to compute the observable charge density from the HF results. Figures-2 and 3 show the charge, proton, neutron and mass densities for the $^{174-206}$Hg isotopes calculated with SkM Skyrme parameterization.

It's evident from Figure-2 (a and b) that the central nuclear charge densities are more depressed when the nuclei become more neutron rich. We note that the central nuclear charge densities gradually decrease as the neutron number increases. This is due to the change in the self-consistent HF potential coming from the additional neutrons. This change in charge density is available in the interior and the surface regions of the nuclei. The contribution of additional neutrons to the density is directly associated to the orbits that filled. In $^{174-206}$Hg, the added neutrons are filled the shells 1g9/2, 1g7/2 and 2d5/2. These orbits are changing the densities in the interior and the surface regions. For this reason the neutron densities in Figure-3 (a and b) are different for the Mo isotopes for all region of *r* (fm). The behavior of the charge densities in the tail region are investigated for the Hg-isotopes in the inset figure of charge and proton densities curves in a logarithmic scale. From these figure we can deduce that the extension of nuclear charge distribution of the neutron-deficient of Hg-isotopes is larger than those of the neutron-rich ones, although the latter isotopes have a larger rms charge radius.

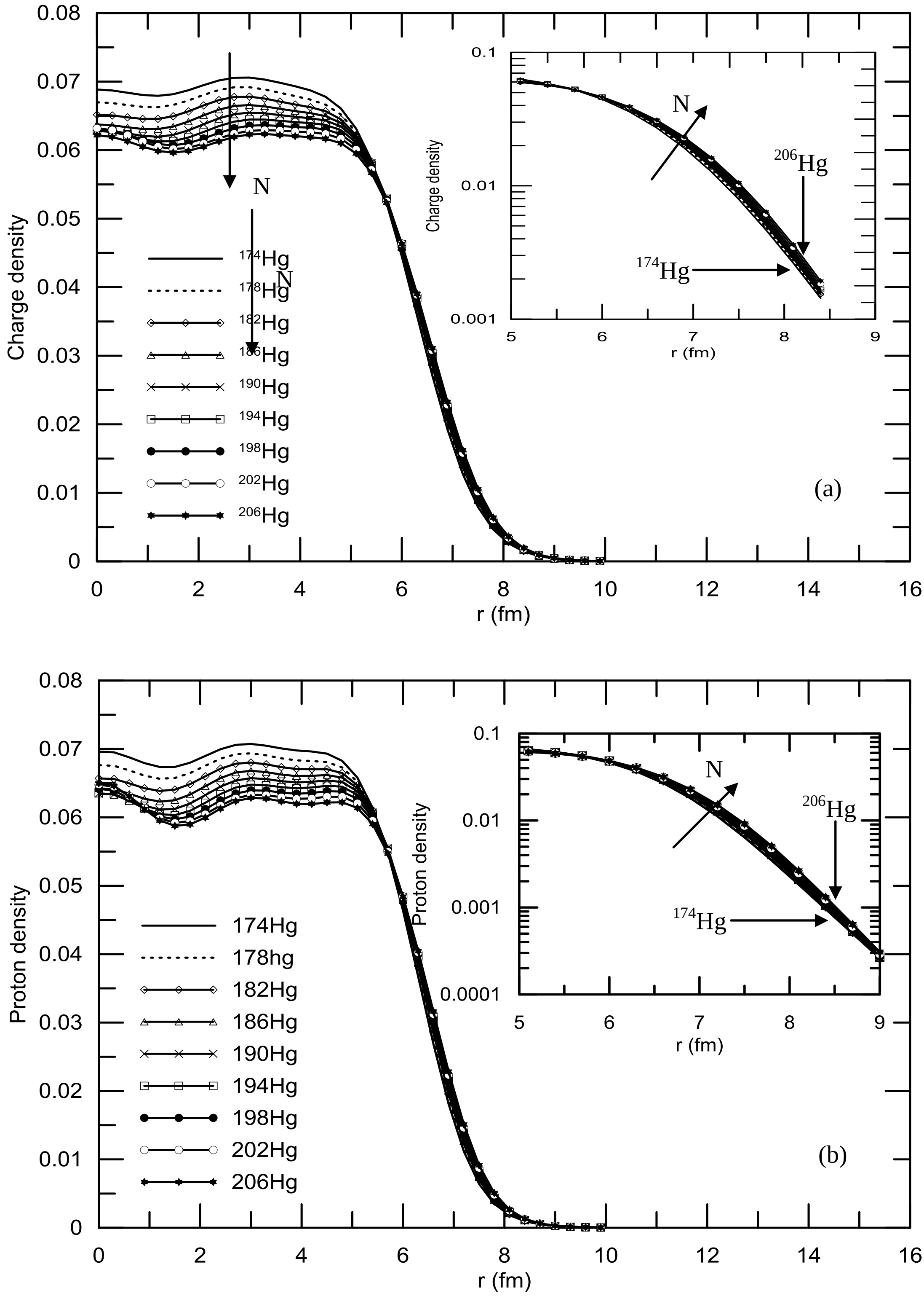

Figure 2-Density variation with neutron number for the Hg isotopes. The inset is in logarithmic scale. Arrows point to the directions in which the neutron number increases. (a) charge density, and (b) proton density.

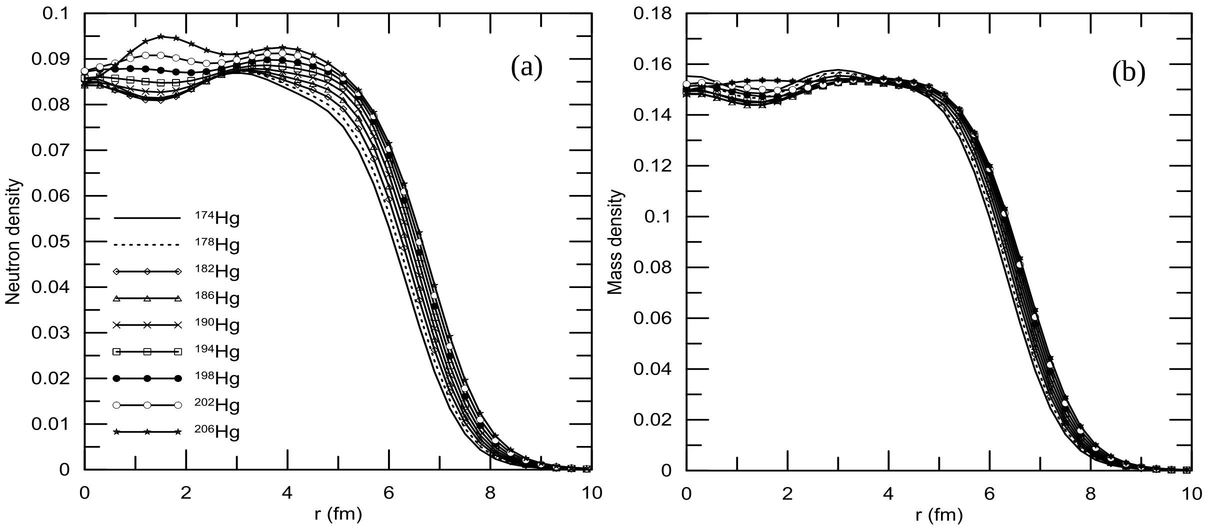

Figure 3-Density variation with neutron number for the Hg isotopes. (a) neutron density and (b) mass density.

The calculated binding energies per particle for $^{174-206}$Hg isotopes as a function of the mass number along with those of experimental data are shown in Figure-4. It may be seen from this figure that calculated binding energies agree remarkably well with the experimental ones [26-29], and are in fact very close to those obtained from interactions SkM for Hg isotopes.

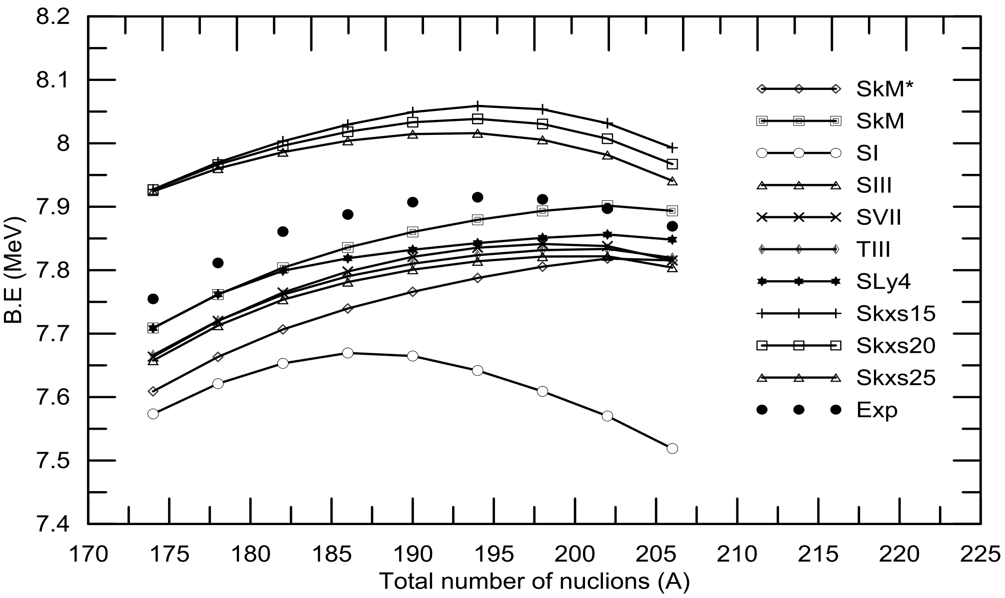

Figure 4-Total binding energy per nucleon for $^{174-206}$Hg isotopes using different Skyrme parameterizations within HF method.

The obtained rms charge radii and neutron skin thicknesses are plotted in Figures-5 and -6. The calculated rms charge radii for $^{174-206}$Hg isotopes obtained with all the selected parameters are compared with the experimental data [30, 31]. The best rms charge radii are obtained with SkM, SLy4 and SkM*. For the neutron skin thickness (t) it can be seen from Fig.6 that the theoretical values of *t* increase with increasing mass number. Its values increased from-0.006 fm (for ^{174}Hg) to 0.189 fm (for ^{206}Hg) by increasing the neutron number with SkM parameterization. The difference between the rms radii of neutrons and protons for $N = Z$ nuclei, or for nuclei with a small neutron excess is negative as one should expect, the Coulomb force pushes the protons away as there is little reliable data for neutron radii, especially for nuclei with a small neutron excess. Since there is little reliable data for neutron radii the comparison of the neutron skin thickness to experiment is difficult.

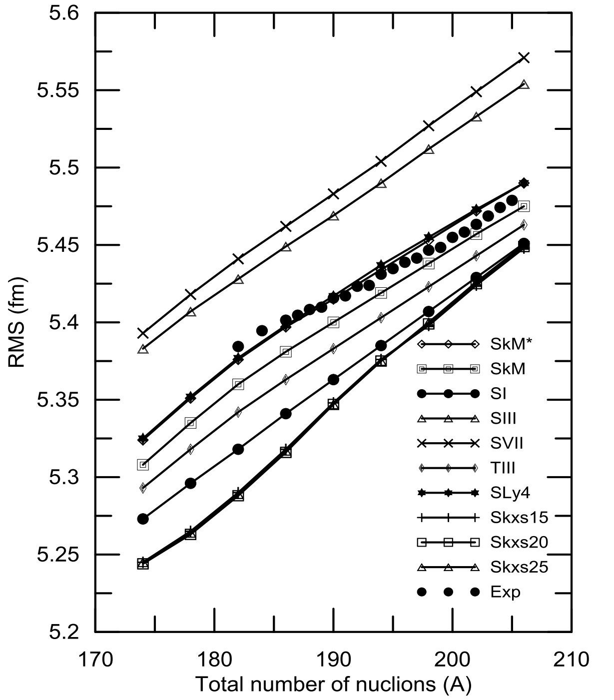

Figurer 5- Calculated rms charge radii for $^{174-206}$Hg isotopes using different Skyrme parameterizations.

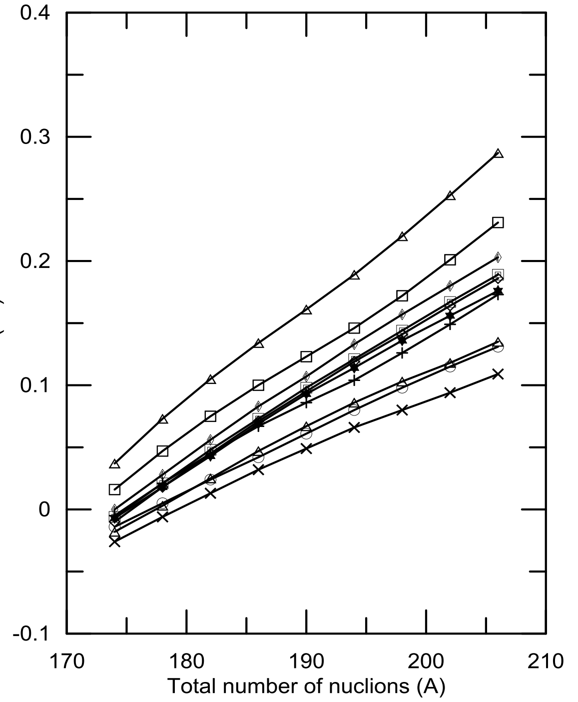

Figure 6- Neutron skin thickness *t* for $^{174-206}$Hg isotopes using different Skyrme parameterizations.

The calculated and experimental rms charge radii as well as the proton and neutron rms radii for the stable ^{204}Hg using different Skyrme parameterizations are shown in Figure-7. It can be seen from this comparison that the best Skyrme parameterizations are the SIII.

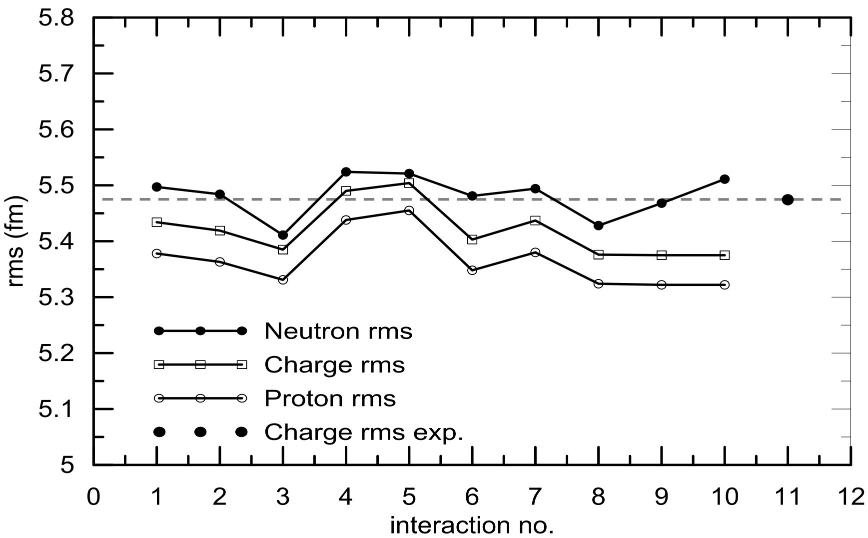

Figure7- Calculated proton and neutron rms radii for ^{204}Hg nucleus using different Skyrme parameterizations.

A study of the charge-density distributions cannot be completely considered without the form factors, since the latter are an important quantities measured experimentally. Thus in Figure-8 for comparison we plotted the charge form factor for the stable ^{204}Hg nucleus using SkM, SkM*, Sly4, Skxs15, Skxs20 and Skxs25 Skyrme parameterizations with the experimental data. The circles for the experimental data are given only over the range of momentum transfers measured experimentally. The plane-wave form factors $|F(q)|^2$ in these figures are associated with the densities in Figures-1 (a) and (b), where the form factors in the range of moderate momentum transfer are sensitive to the change of the tail part of the charge density [32], while small q (fm^{-1}) values inform on the surface shape. It is apparent from Figures-8 (a) and (b) that the theoretical curves (solid) and the experimental ones [33, 34] (filled circles) for ^{204}Hg almost coincide in the range of low and moderate-momentum transfer q (fm^{-1}) out to about 2.5 fm^{-1}. The deviation occurs between the theoretical form factor and the experimental one at high momentum transfers. Since the form factor in this range of momentum transfer is mainly sensitive to the details of the inner part of the charge density distribution, its occurrence indicates that the theoretical charge density distribution has a departure from the experimental one around the center of the nucleus.

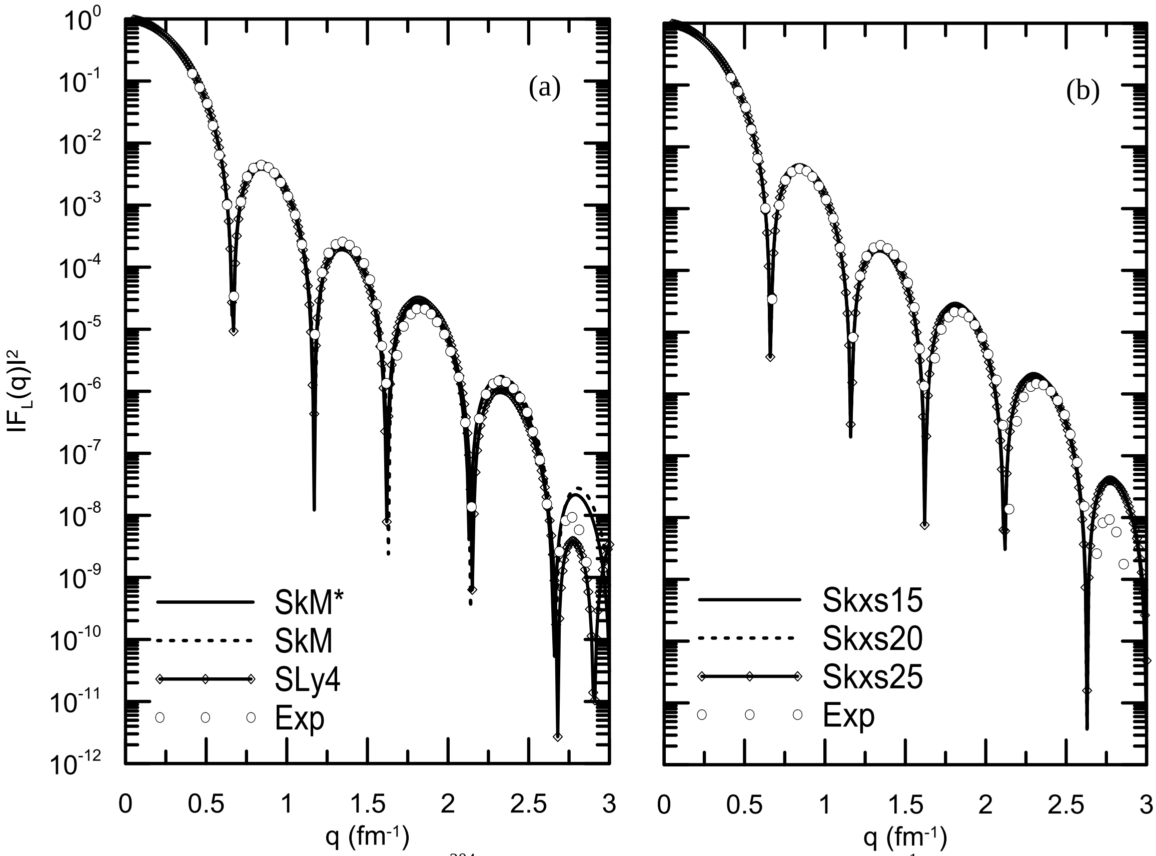

Figure 8- The charge form factor for ^{204}Hg versus momentum transfer q (fm^{-1}) using different Skyrme parameterizations.

Disagreement between experiment and theory above 2.5 fm^{-1} (and the associated discrepancies in the charge densities) might be related to two factors; first, the Skyrme interaction is a low-momentum expansion of the effective interaction, and one must expect the density fluctuations resulting from this approximation to break down at some point. Second, the mesonic-exchange corrections to the charge form factor become increasingly important at higher momentum transfers [35].

We also investigate in Figure-9 the charge form factor for the $^{174-206}$Hg isotopes using the Skxs25 Skyrme parameterization. These figures show the behavior of the charge form factor with the increasing neutron numbers, which is associated with the charge density of the $^{174-206}$Hg isotopes in Figure-2 (a). According to the charge form factors shown in Figure-2 (a), we can see that the minima shift upward and inward with an increasing neutron number. This trend change is due to the variation in the nuclear charge densities, especially the details of the outer parts. This is due mainly to the enhancement of the proton densities in the peripherical region and also to the contribution of the charge distribution of the neutrons themselves.

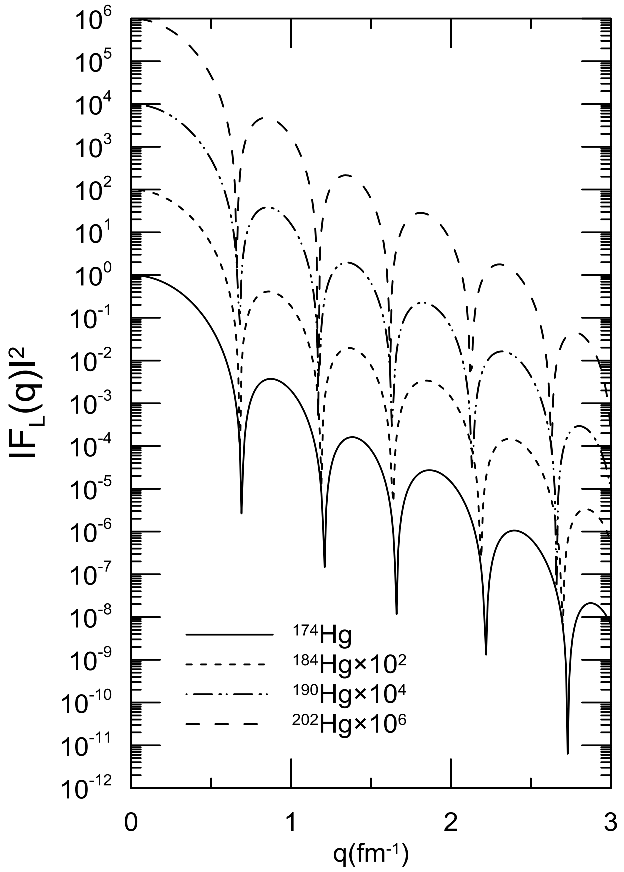

Figure 9- Charge form factors for Hg isotopes versus momentum transfer *q* (fm^{-1}) using Skxs25 Skyrme parameterization.

Conclusions

In the present research, we have investigated the nuclear ground state properties such as the binding energies per particle, charge, neutron and proton density distributions and the associated rms radii, neutron skin thicknesses and charge form factor of $^{174-208}$Hg. The conclusions drawn from this investigation are as follows:

1. The Skyrme-Hartree–Fock method is the useful for calculating of the spherical nuclei because this force is central and has zero range.
2. The B.E of $^{174-206}$Hg calculated using the SHF method with the SkM parameterization is in closer agreement with the experimental data.
3. The calculated charge rms radii for ^{204}Hg with SkM*, SkM and Sly4 parameterizations are closer to the experimental data.
4. The neutron skin thickness *t* have increased with the neutron number for Mo isotopes.
5. The charge form factor obtained using SkM parameter is much more coincide with the experimental data especially in the range of momentum transfer up to 2.5 fm^{-1}.

References

1. Guo-qiang, L.**1990.** Skyrme forces and their applications in low energy nuclear physics. Communications in Theoretical Physics, 13(4), pp: 457-508.
2. Vautherin, D., Brink, D. M.**1972**. Hartree-Fock Calculations with Skyrme's Interaction. I. Spherical Nuclei. *Physical Review* C, 5(3), pp: 626-647.
3. Stone, J.R., Reinhard, P.G. **2007**.The Skyrme interaction in finite nuclei and nuclear matter, *Progress in Particle and Nuclear Physics*, 58, pp: 587-657.
4. Shen, Y. , Ren, Z. **1996**. Skyrme-Haretree-Fock calculation on He, Li and Be isotopes, *Physical Review* C, 54, pp: 1158.

5. Zamrun, M. Usman, I., Aba, L**. 2011**. Investigation of ground state properties of neutron-rich titanium isotopes by the use of SHF+BCS method, *Jurnal Matematika and Sains*, 16(2), pp: 58-64.

6. Tel, E. Okuducu, S. Tanir, G. Akti, N. N. Bolukdemir, M.H. **2008**. Calculation of Radii and Density of $^{7-19}$B Isotopes Using Effective Skyrme Force. *Communications in Theoretical Physics*, 49(3), PP: 696-702.

7. Aytekin, H. Tel, E., Baldik, R. **2008**. Investigation of the ground state features of some excotic nuclei by using effective Skyrme interaction, *Turkey Journal of Physics*, 32, pp: 181-191.

8. Bartel, J. Quentin, P. Brack, M. Guet, C., Hakansson, H. B. **1982**. Towards a better parameterization of Skyrme-like effective forces: A critical study of the SkM force Nuclear Physics A, 386(1), pp: 79-100.

9. Brack, M. Guet, C., Hakansson, H. B. **1985**. Selfconsistent semiclassical description of average nuclear properties a link between microscopic and macroscopic models *Phys. Rep.* 123(5), pp: 275-364.

10. Chabanat, E. Bonche, P. Haensel, P. Meyer, J., Schaeffer, R. **1998**. A Skyrme parameterization from subnuclear to neutron star densities Part II. Nuclei far from stabilities. *Nuclear Physics* A, 635(1-2), pp: 231-256.

11. Li, G. Q. **1991**. A systematic study of nuclear properties with Skyrme forces. *Journal Physics* G. **17(1)**, pp: 1.

12. Tel, E. Sahin, H. M. Kaplan, A. Aydin, A., Altinok, T.**2007**. Investigation of the properties of the nuclei used on the new generation reactor technology systems. *Annals of Nuclear Energy***,** 35(2), pp: 220-227.

13. Tel, E. Okuducu, S. Tanir, G. Akti, N. N. Bolukdemir, M.H. **2008**. Calculation of Radii and Density of $^{7-19}$B Isotopes Using Effective Skyrme Force. Communications in Theoretical Physics, 49(3), PP: 696-702.

14. Alex Brown, B. Shen, G. Hillhouse, G. C. Meng, J., Trzcinska, A. **2007**. Neutron skin deduced from antiprotonic atom data. *Physical Review* C, 76, pp: 034305.

15. Skyrme, T. H.R. **1959**. The effective nuclear potential. *Nuclear Physics* **9**, pp: 615-634.

16. Skyrme, T. H. R.**1956**. The nuclear surface. *Philosophical Magazine*, 1(11), pp: 1043-1054.

17. Bender, M. Heenen, P. H., Reinhard, P. G.**2003**. Self-consistent mean-field for nuclear structure. *Reviews of Modern Physics*, **75**, pp: 121.

18. Aytekin, H., Demirbag, D. **2013**. Investigation of the nuclear properties of ^{181}Ta and $^{182, 183, 184, 186}$W structural materials. *Indian Journal Physics*, **13**, pp: 0253.

19. Tel, E. Aydin, A. Kaplan, A., Sarer, B. **2008**. New calculation method for initial exciton numbers on nucleon induced pre-equilibrium reactions *Physics Review* C, 77 (054605), pp: 1-9.

20. Erler, J. Klupfel, P., Reinhard, P. G.**2011**. Self-consistent nuclear mean field models: example Skyrme-Haretree-Fock, *Journal Physics* G, 38, pp: 033101(1-43).

21. Beiner, M. Flocard, H. Nguyen Van Giai, Quentin, P. **1975**. Nuclear ground-state properties and self-consistent calculations with the Skyrme interaction: (I). Spherical description. *Nuclear Physics* A, 238(1), pp: 29-69.

22. Siiskonen, T. Lipas, P. O., Rikovska J.**1999**. Shell-model and Haretree-Fock calculations for even-mass O, Ne, and Mg nuclei. *Physical Review* C, 60, pp: 034312.

23. Aytekin, H. Tel, E. Baldik, R., Aydin, A.**2010**. New calculation of some ground state features of ^{40}Ca, ^{48}Ca ^{32}S and ^{39}K, *Nuclei International Journal of Modern Physics* E, 19(2), pp: 291–298.

24. Bertulani, C. A.**2007**. Probing nuclear skins and halos with elastic electron scattering *Journal Physics* G, 34, pp: 315-333.

25. Furnstahl, R. J. Price, C. E.**1991**. Charge density differences near ^{208}Pb in relativistic models. *Physical Review* C, 44(2), pp: 895-898.

26. Dreher, B. Friedrich, J. Merle, K. Rothhaas, H. Lührs, G. **1974**. The determination of the nuclear ground state and transition charge density from measured electron scattering data *Nuclear Physics* A, 235(1), pp: 219-248.

27. De Vries, H. De Jager, C. W., De Vries, C. **1987**. Nuclear charge-density-distribution parameters from elastic electron scattering *Atomic Data and Nuclear Data Tables* 36(3), pp: 495-536.

28. Fricke, G. Bernhardt, C. Heiling, K. Schaller, L. A. Shellenberg, L. Shera, E. B., de Jager, C. W. **1995**. Nuclear Ground State Charge Radii from Electromagnetic Interactions, *Atomic Data and Nuclear Data Tables*, 60(2), pp: 177-285.

29. Shen, Y. Zhu, X. F., Ren, Z.**1999**. Deformed-Skyrme-Haretree-Fock calculation of Hg isotopes. *Physical Review* C, 59, pp: 172.

30. Angeli, I. **2004**. A consistent set of nuclear rms charge radii: properties of the radius surface *R*(*N*,*Z*) *Atomic Data and Nuclear Data Tables* 87(2), pp: 185-206.

31. Angeli, I. Marinova, K.P. **2013**. Table of experimental nuclear ground state charge radii: An update Atomic *Data and Nuclear Data Tables*, 99(1), pp: 69-95.

32. Durand, D. Suraud, E., Tamain, B.**2001**. *Nuclear Dynamics in the Nucleonic Regime*. First Edition. IOP publishing, London.

33. Finelli, P. Kaiser, N. Vretenar, D. Weise, W. **2006**. Relativistic nuclear energy density functional constrained by low-energy QCD, *Nuclear Physics* A, 770 (1), pp: 1-31.

34. Richter, W. A., Brown, B. A. **2003**. Nuclear charge densities with the Skyrme Hartree-Fock method *Physical. Review* C, 67, pp: 034317(1-14).

35. Negele J. W., Riska, D.O. **1978**. Pion-exchange contributions to charge densities of closed-shell nuclei. *Physical Review Letters*, 40, pp: 1005.